Coupled Deswelling of Multiresponse Microgels

D. Capriles-González,[†] B. Sierra-Martín,[†] A. Fernández-Nieves,[†,‡,§] and A. Fernández-Barbero*[,†]

Department of Applied Physics, University of Almería, 04120-Almería, Spain, and Department of Physics and HSEAS, Harvard University, Cambridge, Massachusetts 02138

Received: January 15, 2008; Revised Manuscript Received: May 19, 2008

In this article, we study the response of a thermosensitive and ionic microgel to various external stimuli where coupling between different contributions to the total osmotic pressure is needed to describe the observations. We introduce a new Flory solvency parameter χ (T, Q, n) with strong dependence on the network charge, Q, and salt concentration, n. The scaling exponent for the salt-induced deswelling of the microgel is the signature of the coupling between the mixing and ionic osmotic pressures.

1. Introduction

In recent years, "smart" materials have been the focus of considerable interest, from both fundamental and applied perspectives. Polymer microgels are within this category; they respond to specific environmental stimuli by changing their size. Thus, the internal structure, the refractive index, and the mechanical properties of the polymer network change. They are considered superabsorbent materials, as they can absorb solvent up to several hundred times their own weight. They respond rapidly to local environmental variations, an important fact in device miniaturization and microsensor developments.[1] As size changes are accompanied by changes in internal dimensions, microgels have also found application as carriers of therapeutic drugs and as diagnostic agents.[2] They have also been used as microreactors, optically active materials, or for template synthesis of nanoparticles.[3–5]

The swelling or deswelling of this class of materials is induced by modifying the osmotic pressure, which is the end fundamental parameter controlling the size transition. Changes in external variables imply a size change, if such a variable effectively modifies the osmotic pressure. Several studies have described the effects of pH,[6–8] temperature,[9–11] external electric fields,[12] and external stress[13–15] on the microgel swelling behavior. Typical properties of colloidal systems[16–18] have been also reported. This ample spectrum of variables inducing changes in the particle size has prompted the interest in the potential applications of microgels in nano- and biotechnology.[19–24]

Special attention has been paid to poly-*N*-isopropylacrylamide (poly-NIPAM) microgels, as particles based on this monomer exhibit a controlled response to temperature changes,[25,26] and temperature is easy to tune experimentally. A richer response is obtained by copolymerizing NIPAM with ionic monomers, to yield materials that can swell or deswell in response to other environmental parameters, in addition to temperature.[27–33] In many cases, the response of these more complex microgels to a given parameter results from changes in more than one contribution to the total osmotic pressure of the system, π_{total}. This coupling is usually not accounted for, as one typically assumes that certain control parameters only affect a single contribution to π_{total} (i.e., that temperature affects the mixing of the network with the solvent, while charge and salt concentration only modify the ionic contribution to the total osmotic pressure).

In this article, we show that network charge not only affects the ionic distribution of ions inside and outside the gel but also affects the mixing contribution to the total osmotic pressure. To address this coupling, we use poly-NIPAM-(acrylic acid) microgel particles, a system sensitive to temperature, pH, and salt concentration. We account for the experimental results by introducing a modified Flory-solvency parameter, χ (T, Q, n), that depends on temperature, T, as usual, but that also depends on network charge, Q, and salt concentration, n. We find that the size-n scaling exponent is a measure of the coupling between mixing and ionic osmotic pressures.

The outline of this article is as follows: Section 2 is a theoretical background on gel swelling. Particle preparation and the experimental methods are described in sections 3 and 4, respectively. In section 5, we present the experimental results and a discussion based on phenomenological calculations to describe the experiments. Finally, section 6 summarizes the conclusions.

2. Theoretical Basis

Macroscopic equilibrium of polymer gels is attained when the solvent chemical potential is equal inside and outside the gel. Consequently, no net transfer of solvent takes place across the gel−solvent interface and the osmotic pressure within the gel is zero. The osmotic pressure consists of three contributions; these account for the polymer solubility (mixing, π_m), for the network cross-linking (elasticity, π_e), and for its charge (ionic, π_i). The elastic and ionic contributions compete against each other, as the first tries to shrink the gel while the second tries to swell it. The mixing contribution, however, presents an ambivalent behavior; this is determined by the value of the Flory parameter, describing the interaction between polymer and solvent molecules. When the polymer solubility is high, π_m tries to swell the gel, while in the case of a *bad* solvent the mixing is unfavorable and π_m tries to deswell the gel. The Flory−Rehner and Donnan theories describe and quantify the different contributions.[34–38] The mixing and elastic osmotic pressures depend on the polymer volume fraction, ϕ, as:

* To whom correspondence should be addressed. E-mail: afernand@ual.es.
† University of Almería.
‡ Harvard University.
§ Present address: School of Physics, Georgia Institute of Technology, Atlanta, GA 30332.

10.1021/jp8003773 CCC: $40.75
Published on Web 09/05/2008

$$\pi_m = -\frac{N_A kT}{v_s}[\phi + \ln(1-\phi) + \chi\phi^2] \quad (1)$$

$$\pi_e = \frac{N_C kT}{V_0}\left[\left(\frac{\phi}{2\phi_0}\right) - \left(\frac{\phi}{\phi_0}\right)^{1/3}\right] \quad (2)$$

where N_A is the Avogadro number, k is the Boltzmann constant, T is the absolute temperature, and v_s is the molar volume of the solvent. V_0 and ϕ_0 are the volume and polymer volume fraction for a reference state. N_C is the network number of chains that is related with the cross-linker concentration by $N_C = 2N_A[V_0\rho_B]/[M_A + (1/x_A - 1)M_B]$, where ρ_b, M_A, M_B, and x_A are the density, molecular weight, and mole fraction of monomer A or B, as indicated. The Flory parameter is expressed as $\chi = Z[\varepsilon_{ps} - (\varepsilon_{pp} + \varepsilon_{ss})/2]/kT$, with Z the coordination number of a polymer segment and $\varepsilon_{\alpha\beta}$ the interaction energy between polymer (p) and solvent (s) molecules (negative energy indicates attractive interactions).

For nonionic gels, temperature is used to induce the swelling transition through the temperature dependence of χ. The volume fraction, ϕ, is experimentally accessible for isotropic spherical gels through measurements of the gel diameter, D: $\phi/\phi_0 = (D_0/D)^3$, with $D_0 = (6V_0/\pi)^{1/3}$ the size for the reference state, which is usually taken as that of the collapsed gel.

The mixing term shows complex and rich behavior. The *first two terms* in eq 1 account for the increase of entropy when solvent effectively mixes with the gel. It is related to the number of possible conformations a polymer chain can adopt. The *third term* contains the polymer−solvent interaction, χ. It is of enthalpic nature and determines the solvent quality. Figure 1a illustrates the total osmotic pressure as a function of polymer volume fraction. Also shown are the purely entropic and enthalpic contributions; the first tries to swell the gel, whereas the latter, for $\chi = 0.9$, tries to deswell it. The net mixing term contributes to either case depending on ϕ. In Figure 1b, curves for different χ values are shown. There are two different behaviors: (i) for high polymer solubility ($\chi < 0.5$), the osmotic pressure increases monotonously with ϕ, always favoring gel swelling; (ii) π_m exhibits a minimum on the deswelling region (negative values of π_m) for low polymer solubility ($\chi > 0.5$). The mixing contribution always tries to swell the gel for high enough polymer densities, while for smaller ϕ, it inverts its effect contributing to gel collapse.

The network elasticity, eq 2, always contributes to gel deswelling. It is asymmetric in nature and clearly nonlinear with ϕ. At low polymer densities, an increase in ϕ induces a sharp increase in π_e; this is more pronounced for a larger number of chains. In the vicinity of $\phi = 0.5$, it is practically independent of the polymer density. Beyond this point, π_e slightly reduces its deswelling ability. For very low polymer volume fractions, the solvent inside and outside the network becomes indistinguishable and the osmotic pressures associated to all contributions vanish.

For ionic gels, an additional contribution describing the presence of charge has to be considered; it manifests through direct Coulombic repulsions among polymer chains and by the effect of the ion distribution inside and outside the gel.[36] Within the weak screening limit ($\kappa R < 1$, with R the size of a polymer chain and κ the inverse of the Debye length), the electrostatic repulsion does not work and the latter effect dominates: The network charge sets a constant electrostatic potential (Donnan potential, U), driving the redistribution of ions inside and outside the gel. The result is given by a Boltzmann distribution, $n_i/n_i^* = \exp[-z_i eU/kT]$, with n_i and n_i^* the concentration of the i-ionic species inside and outside the gel, respectively, z_i the ion valence, and e the elementary charge. As a result of this unequal ion distribution, an osmotic pressure is established inside the gel: $\pi_i = N_A kT\sum_i(n_i - n_i^*)$.

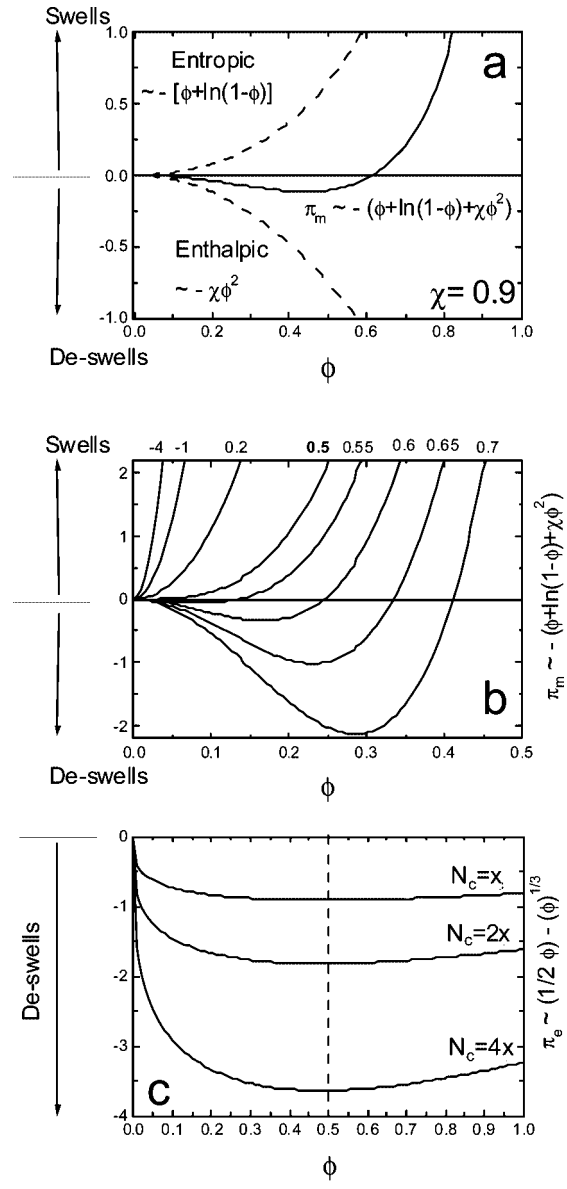

Figure 1. (a) Entropic and enthalpic contributions to the total mixing osmotic pressure. (b) Mixing term for different polymer solubilities; χ values are indicated at the top axis. (c) Network elasticity term. For this calculation, $x = 9.89 \times 10^6$ chains/particle, which corresponds to the N_C experimental value.

In the weak screening limit, the ionic osmotic contribution depends on the ionic concentration, n (for high enough ionic concentration, $Q/V < n$, with Q being the gel charge), as:[36]

$$\pi_i = \frac{kTN_A}{4n}\left(\frac{\phi}{\phi_0}\right)^2\left(\frac{Q}{V_0}\right)^2 \quad (3)$$

When the salt concentration is lower than the network charge density, the number of counterions is equal to the network charges and π_i is independent of salt concentration. In the opposite case, the excess salt ions lowers the ionic concentration difference inside and outside the gel and π_i decreases with increasing n.[36,38]

The different contributions to the total osmotic pressure do not work independently. Their relation is given by the equation of state:

$$\pi_{total} = \pi_m + \pi_e + \pi_i = 0 \quad (4)$$

Changes in particle size modify the different contributions to the total osmotic pressure, so that thermodynamic equilibrium is attained. Figure 2a plots the mixing, elastic, and ionic terms against salt concentration for $\chi = 0.2$. As can be seen, the increase in ionic concentration directly acts on the ionic contribution, since $\pi_i \approx 1/n$. The system responds by increasing the particle volume fraction, or equivalently, by decreasing its size. As a result, π_m increases and π_i decreases; this occurs so that $\pi_{total} = 0$.

When the polymer solubility is lower ($\chi = 0.6$ in Figure 2b), the mixing contribution cannot compensate the ionic osmotic pressure reduction induced by increasing n. It even adds to the elastic contribution to deswell the gel. The only possibility to fulfill the equilibrium equation is the ionic self-compensation. π_i decreases with ion concentration but also increases with the volume fraction, ($\pi_i \approx \phi^2/n$). The system must increase ϕ as necessary to compensate the reduction of osmotic pressure due to $1/n$ as well as the negative elastic contribution and the increasing negative mixing term. This is why π_i increases against n. Beyond certain n value, π_m reduces its strength to deswell the gel (minimum at the inset in Figure 2b) and π_i stops increasing. The ionic contribution to equilibrium reaches a maximum. For higher n values, the ionic term has to compensate only the deswelling elastic term. The necessary volume fraction increment to reach equilibrium is smaller, and the osmotic pressure reduction due to increasing n provokes a net π_i decreasing.

3. Experimental System

Particles are synthesized by free-radical emulsion polymerization in the absence of surfactant. The system is based on NIPAM, acrylic acid (AA, 8 wt %), and *N*,*N*′-methylenebisacrylamide (BA, 4 wt %), as cross-linker. The monomer NIPAM (10.56 g, Aldrich), the comonomer AA (0.96 g, Aldrich), and the cross-linker BA (0.48 g, Aldrich) react in the presence of azobiscyanopentanoic acid initiator. The reaction is carried out in a three-necked vessel fitted with a stirred paddle, a reflow condenser, and a nitrogen inlet tube. The vessel is filled to 800 mL using deionized water and immersed in a water bath at 70 °C. The reaction mixture is stirred at 350 rpm for 20 min with nitrogen purge to exclude dissolved oxygen. The initiator (0.48 g, Aldrich) is then added to initiate the reaction. It is maintained for 16 h under nitrogen atmosphere. All materials were reagent grade and used without further purification.

The dispersion is allowed to cool and then it is extensively dialyzed against distilled water to remove impurities. The dialysate is changed twice daily until the conductivity is reduced to 1 μS/cm. A dispersion of poly-(NIPAM-AA) particles with $N_C = 9.89 \times 10^6$ chains/particle is obtained. The inset in Figure 3 shows a transmission electron microscopy (TEM) image of the particles. The particles are spherical and the suspension monodisperse. The average diameter determined by DLS for collapsed particles is 388 ± 10 nm.

4. Experimental Methods

Conductimetric and Potentiometric Titrations. Simultaneous titrations are performed to access the total charge and the charge-pH dependence, respectively. Measurements are carried out using a cell supporting both pH and conductivity electrodes as well as a nitrogen inlet to titrate in the absence of air. A computer-controlled dispenser of ±1-μL sensitivity feeds sodium hydroxide or hydrochloric acid to titrate the samples.

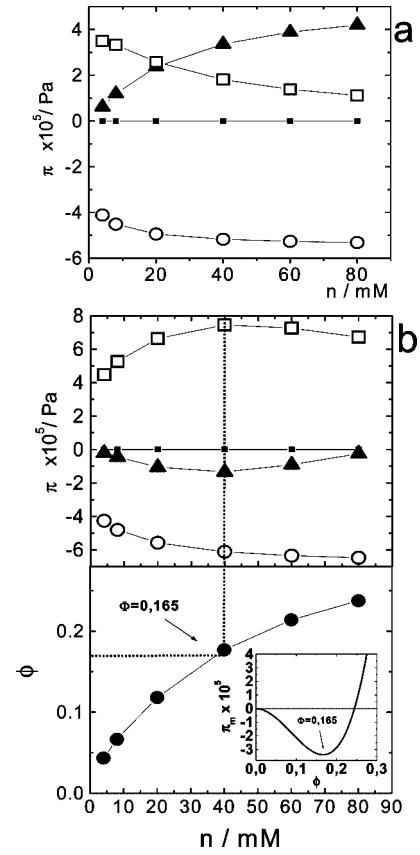

Figure 2. Osmotic pressures against salt concentration (○) π_e, (□) π_i, (▲) π_m in equilibrium (the total osmotic pressure ■ is zero for all n). (a) High solubility, $\chi = 0.2$. (b) Low solubility, $\chi = 0.6$. Volume fractions at equilibrium are also plotted. The mixing term is represented in the inset. Calculations for these graphs correspond to $Q = 3.85 \times 10^{-12}$ C/particle, $d_0 = 388$ nm, $N_C = 9.89 \times 10^6$ chains/particle, and $T = 17$ °C.

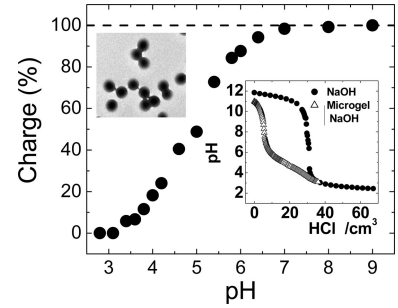

Figure 3. Microgel charge-pH dependence. For pH ≥ 7, the acrylic acid molecules are completely ionized and the particle bears the maximum charge, $Q = 3.85 \times 10^{-12}$ C/particle. The insets show a TEM image of the colloidal suspension and the microgel and reference potentiometric titrations.

Temperature is set at 25 ± 1 °C. Gentle stirring diminishes temperature and concentration gradients.

Dynamic Light Scattering. The size of the particles is determined using dynamic light scattering. A Malvern 4700 system equipped with a 632.8-nm wavelength He−Ne laser is employed, with the scattering angle set to 40°. Temperature is controlled with a precision of 0.1 °C using both a Peltier cell and external bath acting through the sample cell. Sample temperature is equilibrated for 20 min before the size measurement. Low particle concentrations are used to reduce the effect of colloidal interactions and to warrant simple scattering conditions. The mean diffusion coefficient is derived from the

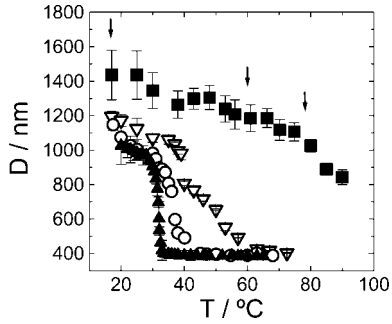

Figure 4. Effect of charge on the microgel response to temperature. (▲) Uncharged, (○) pH = 4.1 (20% charged), (▽) pH = 5.6 (75% charged), and (■) pH = 7.8 (100% of charge). The arrows indicate the chosen temperatures for the experiments in Figure 8.

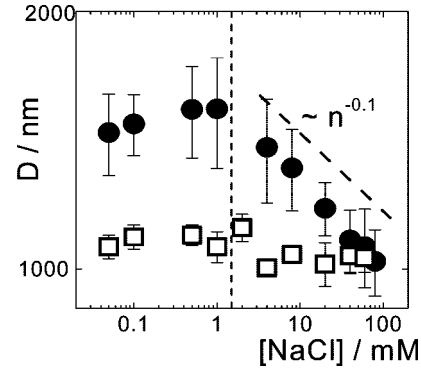

Figure 5. Particle size D versus salt concentration n. pH = (●) 4.1 and (□) 7.8. As can be observed, the ionic concentration has an effect only when the particle charge is large. In this case, for $n > Q/V$, we find that $D \approx n^{-0.1}$. The temperature is set to 17 °C in these experiments.

intensity autocorrelation function using cumulant analysis and converted into mean particle size via the Stokes−Einstein equation for spherical particles. Every size value is obtained from the average of five measurements. The polydispersity is estimated to be $b/\Gamma^2 < 0.08$ (highly monodisperse samples) in every case. The polydispersity index b/Γ^2 was calculated from the field autocorrelation function, $g_1(q, \tau) = \exp(-\Gamma\tau)(1 + b\tau^2/2! + c\tau^3/3! + ...)$, where Γ is the average rate decay, $\Gamma = D \cdot q^2$, where D is the diffusion coefficient.

5. Results and Discussion

Microgel Charge. The charge carried by the microgel particles is determined by inverse conductometric titration using HCl as the titration agent. Three typical regions are distinguished: neutralization of the excess OH^- ions, neutralization of weak acid groups, and excess of H^+ ions. No strong acid groups were detected in the direct titration, confirming that all ionizable groups have a weak character; they are carboxyl groups arising from the ionization of the AA and initiator. The total charge per particle obtained was $Q = 3.85 \times 10^{-12}$ C/particle. Details about charge determination can be found elsewhere.[6,26] To determine the charge-pH dependence, inverse potentiometric titrations are performed. The inset in Figure 3 shows the titrations of both a microgel suspension and a reference solution of NaOH. At high pH, there is excess of H^+ ions and both curves overlap. The particle charge at every pH is determinated from the difference between the microgel and reference curves. This is shown in Figure 3, where we plot the total charge in % versus pH. As expected, the total charge increases with pH because of the ionization of AA groups. All groups are ionized for pH ≈ 7.

Temperature-Induced Deswelling. The particle size is monitored against temperature for different charge states (set using HCl and NaOH). Figure 4 plots four representative $D-T$ curves corresponding to uncharged, 20, 75, and 100% of the total charge. As expected, microgel particles are sensitive to temperature and pH changes. For uncharged NIPAM-AA microgels, D decreases gradually with temperature. A sharp volume transition is obtained reminiscent of that typically observed for pure NIPAM particles.[39,40] The transition temperature is ~32 °C, in agreement with the lower solubility critical temperature of the neutral NIPAM−water system.[41] The process is thermoreversible without any significant hysteresis.

Charge activation affects the microgel size and shrinking process. The presence of charge (20 and 75%) adds a contribution to the total osmotic pressure trying to swell the particles. The transition shifts to higher temperatures and broadens. The establishment of a Donnan potential inside the particles induces an uneven distribution of ions inside and outside the microgels. This results in an ionic osmotic pressure that competes against the mixing contribution that tries to shrink the gels resulting in the observed phenomenology. Our results agree with previous observations on poly-NIPAM-AA micro[32] and macrogels.[42,43] For fully charged particles, the attractive hydrophobic interaction trying to collapse the microgel at high temperatures is not strong enough to overcome the increased Donnan osmotic pressure. As a result, the particles do not reach the shrunken state, even at 90 °C.

Note that the particle size is sensitive to the network charge, as expected; it increases with increasing Q. In particular, at low temperatures, when the microgels are highly swollen, the network mechanical swelling limit has not been reached, as there is extra swelling induced by charging the network.

Salt-Induced Deswelling. To study the relevance of the ionic contribution on particle deswelling, we fix the temperature to $T = 17$ °C. We vary the strength of this osmotic pressure by tuning the pH (network charge) and the ionic concentration. We consider two charge states corresponding to low and completely ionized networks. Figure 5 plots the hydrodynamic diameter as a function of salt concentration at pH 4.1 (20% of the maximum charge) and pH 7.8 (maximum charge). At pH 4.1, the particle size does not change significantly with salt concentration. The Donnan potential is very weak, and there is no significant ion redistribution inside and outside the microgels. The ionic term in the equilibrium equation is not relevant in this particular case. At pH 7.8, the strengths of both mixing and ionic contributions are high. Two regions are distinguished in the weak screening limit. At low salt concentrations, there is no significant variation of the particle size with n; this is in agreement with the theoretical expectations (eq 3). For salt concentrations above the microgel charge density, the experimental particle size scales with n as a power law within the experimental n-range covered. We find that $D \approx n^{-0.1}$. In this region, the microgel deswells as a result of the decreasing ionic osmotic pressure (eq 3).

Comparison with Theoretical Predictions. The Flory−Rehner−Donnan theory is employed to describe particle deswelling. In a first approximation, we assume that the different contributions to the total osmotic pressure are decoupled. The control parameters are then $\chi(T)$, N_C, Q, and n; they only affect the values of π_m, π_e, and π_i, respectively. Figure 6 shows the theoretical expectations for particle deswelling with salt concentration, for several values of the Flory parameter. The theoretical $D \approx n$ deswelling curves were determined using eqs

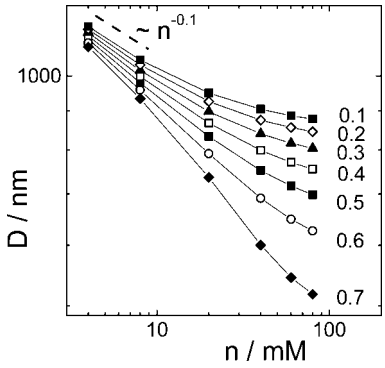

Figure 6. Theoretical diameter against ion concentration for a fully charged polymer network. $Q = 3.85 \times 10^{-12}$ C/particle. and $N_C = 9.89 \times 10^6$ chains/particle (experimental values). The reference particle size $D_0 = 388$ nm was set as the smallest experimental diameter. Curves correspond to different polymer Flory parameters, ranging from 0.1 to 0.7 and corresponding to mixing contributions trying to swell or shrink the microgel.

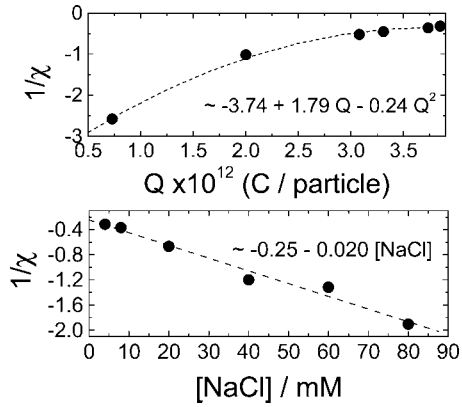

Figure 7. Flory parameter against (a) particle charge (for [NaCl] = 5 mM) and (b) salt concentration (for a 100% charged network). Temperature is set to 17 °C.

1–4. The experimental parameters Q, N_C, and T were used as inputs to perform the calculations. The reference particle size is taken as the collapse size, which we estimate with DLS.

None of the curves reproduce the observed $D-n$ dependence, as the deswelling rate decreases with increasing n. The classical correction $\chi(\phi) \approx \Sigma\chi_i\phi_i$ with i [0,∞] is not suitable for describing the experiment−theory disagreement since it is only relevant for high polymer volume fractions. In the experimental situation ϕ [0.022−0.235] and this correction is not significant.

To describe the experiments, the size should be smaller than predicted as n increases. A decreasing solubility with increasing salt concentration could account for the discrepancy. In this same direction, we must also account for the fact that the network charge modifies the polymer−solvent solubility; it favors mixing of both components.

Coupling between Osmotic Pressure Contributions. To investigate the connections among the control parameters, we determine the solubility, χ, against particle charge and salt concentration. Calculations are performed using the equation of state (eq 4) for the experimental volume fraction, network charge, and salt concentration ranges, extracted from Figures 4 and 5.

Figure 7 shows a nonlinear increasing and decreasing solubility for increasing charge and salt concentration, respectively. The negative values of the Flory parameter indicate extremely high polymer solubilities. The charging of the network and the presence of salt in the solvent not only swell or deswell

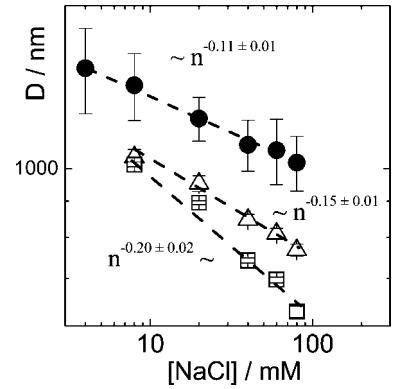

Figure 8. Experimental deswelling scaling laws for different temperatures for a fully charged microgel. T = (●) 17, (△) 60, and (□) 78 °C. Volume fractions, ϕ, are within the range 0.022−0.055 at $T = 17$ °C, 0.052−0.129 at $T = 60$ °C, and 0.056−0.235 at $T = 78$ °C.

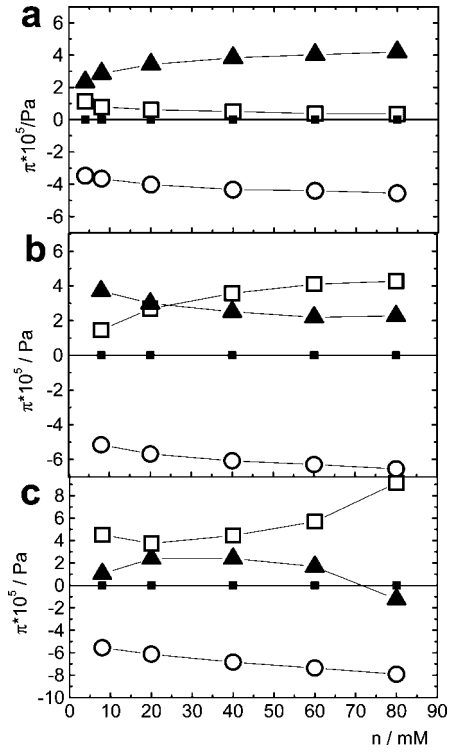

Figure 9. Osmotic pressures against counterion concentration, accounting for the dependence of $\chi(n)$: (○) π_e, (□) π_i, (▲) π_m under the equilibrium condition (the total osmotic pressure ■ is constant). Calculations correspond to the fully charged network, $Q_p = fNc = 3.85 \times 10^{-12}$ C/particle, $d_0 = 388$ nm, and $N_C = 9.89 \times 10^6$ chains/particle. T = (a) 17, (b) 60, and (c) 78 °C.

the microgel through the ionic contribution to the total osmotic pressure, but also affect the mixing part through χ. There is thus coupling between the different contributions to π_{total}. The magnitudes $1/\chi$ (Q) and $1/\chi$ (n) were obtained by fitting the experimental data and are shown in Figure 7.

Both salt and network charge modify the mixing free energy: (i) Salt disturbs the structured water that surrounds the hydrophobic isopropyl groups of the NIPAM network.[44,45] The ions displace water molecules and reduce the local order inducing the network collapse. The net entropy thus increases and $\chi \approx |\Delta S|/k$ rises. (ii) Charged groups lead to the opposite effect. The local electrostatic field orders the water dipoles around ionic charges. The net entropy decreases and polymer solubility increases; this results in swelling of the network.

Scaling Exponents and the Dominant Deswelling Mechanism. Experimental deswelling curves at three different temperatures (see arrows in Figure 4) for a fully charged microgel are plotted in Figure 8. As can be observed, within the experimental n-range, D decreases with n as a power law. The exponent increases in absolute value from 0.11 to 0.15 to 0.20 as the temperature is increased from $T = 17$ °C to $T = 60$ °C to $T = 78$ °C, respectively. To understand these results, we plot in Figure 9 how the different contributions to π_{total} change as a function of n for these experiments. We thus consider a completely charged microgel with a Flory solvency parameter χ (T, Q, n) that depends not only on T, but also on Q and n. Calculations were performed using eqs 1–4 and the experimental n, χ, and ϕ as input data.

At high temperatures (Figure 9c), the ionic term dominates particle swelling[36] and the scaling exponent reduces even more to reach $\alpha = -0.2$. At low temperatures (Figure 9a), the mixing term controls particle deswelling showing a scaling power law $D = n^{\alpha}$ with exponent $\alpha = -0.1$. For increasing temperature (Figure 9b), the ionic term becomes comparable to the mixing one, both contributing to particle swelling.[46] The exponent α then decreases to -0.15. For even higher temperature (Figure 9c), the ionic term dominates particle swelling[47] and the scaling exponent reduces even more to reach $\alpha = -0.2$. For pure ionic gels, the mixing term does not contribute to swelling and the gel size is controlled by the competition between elastic and ionic terms. In this case, decreasing size with salt is predicted[48] to scale as $D \approx n^{-0.2}$. This limit has been experimentally checked for fully charged vinilpyridyne microgels.[23] The present experiments are consistent with this behavior, and the decreasing rate typical for pure ionic networks is reached when ionic contribution dominates (even when the mixing contribution is not null at all).

6. Conclusions

The response of a thermosensitive and ionic microgel to multiple external stimuli is controlled by coupled contributions to the total osmotic pressure. A multidependent Flory-solvency parameter χ (T, Q, n) describes the results. The value of the scaling exponent, $D \approx n^{\alpha}$, becomes the signature of the interaction controlling particle deswelling: $\alpha = -0.1$ for a mixing influenced process and $\alpha = -0.2$ for a charge-controlled process. The proximity of the exponent to one of these two limits weights the relevance of the mixing or ionic contributions to particle deswelling.

Acknowledgment. This work was supported by Ministerio de Ciencia y Tecnologı´a (Spain) under project MAT2006-13646-C03-02 and Junta de Andalucı´a under "Excellence Project": FQM-02353.

References and Notes

(1) Nayak, S.; Lyon, L. A. *Angew. Chem., Int. Ed.* **2005**, *44*, 7686–7708.
(2) Vinogradov, S. V. *Curr. Pharm. Des.* **2006**, *12*, 4703–4712.
(3) Das, M.; Zhang, H.; Kumacheva, E. *Annu. Rev. Mater. Res.* **2006**, *36*, 117–142.
(4) Kim, J.; Nayak, S.; Lyon, L. A. *J. Am. Chem. Soc.* **2005**, *127*, 9588–9592.
(5) Kim, J.; Serpe, M. J.; Lyon, L. A. *Angew. Chem., Int. Ed.* **2005**, *44*, 1333–1336.
(6) Fernandez-Nieves, A.; Fernandez-Barbero, A.; Vincent, B.; de las Nieves, F. J. *Macromolecules* **2000**, *33*, 2114–2118.
(7) Fernandez-Nieves, A.; Fernandez-Barbero, A.; de las Nieves, F. J. *Langmuir* **2000**, *16*, 4090–4093.
(8) Fernandez-Nieves, A.; Fernandez-Barbero, A.; de las Nieves, F. J. *Phys. Rev. E* **2001**, *63*, 041404.
(9) Pelton, R. *Adv. Colloid Interface Sci.* **2000**, *85*, 1–33.
(10) Fernandez-Barbero, A.; Fernandez-Nieves, A.; Grillo, I.; López-Cabarcos, E. *Phys. Rev. E* **2002**, *66*, 051803.
(11) Sierra-Martin, B.; Choi, Y.; Romero-Cano, M. S.; Cosgrove, T.; Vincent, B.; Fernandez-Barbero, A. *Macromolecules* **2005**, *38*, 10782–10787.
(12) Fernandez-Nieves, A.; Fernandez-Barbero, A.; de las Nieves, F. J.; Vincent, B. *J. Phys.: Condens. Matter* **2000**, *12*, 3605–3614.
(13) Fernandez-Nieves, A.; Fernandez-Barbero, A.; Vincent, B.; de las Nieves, F. J. *J. Chem. Phys.* **2003**, *119*, 10383–10388.
(14) Bradley, M.; Ramos, J.; Vincent, B. *Langmuir* **2005**, *21*, 1209–1215.
(15) Routh, A.; Fernandez-Nieves, A.; Bradley, M.; Vincent, B. *J. Phys. Chem. B* **2006**, *110*, 12721–12727.
(16) Tirado-Miranda, M.; Schmitt, A.; Callejas-Fernandez, J.; Fernandez-Barbero, A. *Colloids Surf., A* **2000**, *162*, 67–73.
(17) Puertas, A. M.; Fernandez-Barbero, A.; de las Nieves, F. J. *Comput. Phys. Commun.* **1999**, *121*, 353–357.
(18) Sierra-Martin, B.; Romero-Cano, M. S.; Fernández-Barbero, A. *Colloid Polym. Sci.* **2005**, *284*, 941–945.
(19) Li, J.; Hong, X.; Liu, Y.; Li, D.; Wang, Y. W.; Li, J. H.; Bai, Y. B.; Li, T. J. *Adv. Mater.* **2005**, *17*, 163–166.
(20) Takeoka, Y.; Watanabe, M. *Adv. Mater.* **2003**, *15*, 199–201.
(21) Lee, Y. J.; Braun, P. V. *Adv. Mater.* **2003**, *15*, 563–566.
(22) Hu, Z.; Xia, X. *Adv. Mater.* **2004**, *16*, 305–309.
(23) Fernandez-Nieves, A.; Fernandez-Barbero, A.; de las Nieves, F. J. *J. Chem. Phys.* **2001**, *115*, 7644–7649.
(24) Fernandez-Nieves, A.; van Duijneveldt, J. S.; Fernandez-Barbero, A.; Vincent, B.; de las Nieves, F. J. *Phys. Rev. E* **2001**, *64*, 051603.
(25) Hirotsu, S.; Hirokawa, Y.; Tanaka, T. *J. Chem. Phys.* **1987**, *87*, 1392–1995.
(26) Sierra-Martin, B.; Romero-Cano, M. S.; Fernández-Nieves, A.; Fernández-Barbero, A. *Langmuir* **2006**, *22*, 3586–3590.
(27) Snowden, M. J.; Chowdhry, B. Z.; Vincent, B.; Morris, G. E. *J. Chem. Soc., Faraday Trans.* **1996**, *92*, 5013–5016.
(28) Jones, M. S. *Eur. Polym. J.* **1999**, *35*, 795–801.
(29) Makino, K.; Agata, H.; Ohshima, H. *J. Colloid Interface Sci.* **2000**, *230*, 128–134.
(30) Lopez-Cabarcos, E.; Mecerreyes, D.; Sierra-Martin, B.; Romero-Cano, M. S.; Strunz, P.; Fernandez-Barbero, A. *Phys. Chem. Chem. Phys.* **2004**, *6*, 1396–1400.
(31) Daly, E.; Saunders, B. R. *Phys. Chem. Chem. Phys.* **2000**, *2*, 3187–3193.
(32) Kratz, K.; Hellweg, T.; Eimer, W. *Colloid Surf., A* **2000**, *170*, 137–149.
(33) Hoare, T.; Pelton, R. *Polymer* **2005**, *46*, 1139–1150.
(34) Flory, P. J. *Principles of Polymer Chemistry*; Cornell University Press: London, 1953.
(35) Flory, P. J.; Rehner, J., Jr. *J. Chem. Phys.* **1943**, *11*, 521–526.
(36) Barrat, J.-L.; Joanny, J.-F.; Pincus, P. *J. Phys. II* **1992**, *2*, 1531–1544.
(37) Hiemenz, P. C.; Rajagopalan, R. *Principles of Colloid and Surface Chemistry*; Marcel Dekker: New York, 1997.
(38) Shibayama, M.; Tanaka, T. Volume Phase Transition and Related Phenomena of Polymer Gels. In *Responsive Gels: Volume Transitions*; Dusek, K., Ed.; Springer: Germany, 1993.
(39) Sierra-Martin, B.; Romero-Cano, M. S.; Cosgrove, T.; Vincent, B.; Fernandez-Barbero, A. *Colloid Surf., A* **2005**, *270*, 296–300.
(40) Kratz, K.; Hellweg, T.; Eimer, W. *Polymer* **2001**, *42*, 6631–6639.
(41) Wu, J.; Zhou, B.; Hu, Z. *Phys. Rev. Lett.* **2003**, *90*, 48304.
(42) Kawasaki, H.; Sasaki, S.; Maeda, H. *J. Phys. Chem. B* **1997**, *101*, 4184–4187.
(43) Kawasaki, H.; Sasaki, S.; Maeda, H. *J. Phys. Chem. B* **1997**, *101*, 5089–5093.
(44) Annaka, M.; Amo, Y.; Sasaki, S.; Tominaga, Y.; Motokawa, K.; Nakahira, T. *Phys. Rev. E* **2002**, *65*, 031805.
(45) Lopez-Leon, T.; Fernandez-Nieves, A. *Phys. Rev. E* **2007**, *75*, 011801.
(46) The ionic contribution is more relevant at low ϕ. It decreases with ion concentration, and the mixing term takes the baton from the ionic contribution. Thus, curves cross in Figure 9b.
(47) At very low ion concentration, the increase of n induces a decrease of π_i, and π_m compensates it. For increasing ion concentration, the mixing term cannot equilibrate and the ionic term self-compensates, increasing the value to compete against the elastic deswelling contribution and even against the mixing term for higher ϕ values.
(48) Pincus, P. *Macromolecules* **1991**, *24*, 2912–2919.

JP8003773